PHYSICAL REVIEW E **78**, 051201 (2008)

Relation of water anomalies to the excess entropy

Zhenyu Yan,[1] Sergey V. Buldyrev,[1,2] and H. Eugene Stanley[1]
[1]*Center for Polymer Studies and Department of Physics, Boston University, Boston, Massachusetts 02215, USA*
[2]*Department of Physics, Yeshiva University, 500 West 185th Street, New York, New York 10033, USA*

(Received 14 August 2008; published 19 November 2008)

Using the five-site transferable intermolecular potential (TIP5P) we perform molecular dynamics simulations to investigate the relationship between the excess entropy and anomalies of water. We find that the two-body excess entropy is an ideal quantity to predict the regions of structural, dynamic, and thermodynamic anomalies of water in its pressure-temperature and density-temperature phase diagrams. From the excess entropy we can also predict the location of the Widom line, associated with the hypothesized liquid-liquid critical point in supercooled water.

DOI: 10.1103/PhysRevE.78.051201 PACS number(s): 61.20.−p, 05.20.Jj

The anomalies of water are related to its local tetrahedral structure. It is hypothesized that at very low temperatures T, water undergoes a phase transition between low density liquid (LDL) with large empty space around the tetrahedrally coordinated molecules and the high density liquid (HDL) in which additional molecules enter the first coordination shell and weaken its tetrahedrality [1,2]. When the local structure is characterized by translational and orientational order parameters, the regions of anomalous behavior of these parameters, and also density ρ and diffusivity D, are enclosed in each other on the T-ρ phase diagram, thus forming a cascade of anomalies [3]. This fact indicates that various anomalies are not independent but stem from the same origin, namely the critical point which terminates the hypothesized LDL-HDL phase transition coexistence line [1]. The continuation of this coexistence line into the one-phase region forms the Widom line [4]. Response functions, such as isothermal compressibility K_T and isobaric heat capacity C_P, have maxima near the Widom line [5]. The Widom line is also related to the dynamic crossover of water [4,6].

The models interacting with a repulsive spherically symmetric potential [7–14] display waterlike anomalies despite lack of highly directional hydrogen bonds, because the hard core of these potentials mimics the rigid first shell of water, while the repulsive soft core mimics the energy barrier that water molecules need to overcome to migrate from the second shell toward the first shell [9]. The repulsive soft core creates empty space in the structure which can be reduced by compression or heating, and this mimics [9] the LDL-HDL structural transition in water although there is no orientational interaction and tetrahedral structure in these models. These two-scale repulsive potentials also exhibit waterlike structural anomalies [9]. As a measure of structure, Ref. [8] used excess entropy,

$$S_{\mathrm{ex}} \equiv S - S_{ig} \equiv S + k_B \ln \rho - c(T), \qquad (1)$$

defined as the difference between S, the total entropy of a fluid, and $S_{ig} \equiv -k_B \ln \rho + c(T)$, the ideal gas entropy, where k_B is the Boltzmann constant. Reference [8] successfully predicts the density and dynamic anomaly regions for a repulsive simple liquid with waterlike anomalies. The connection between two-body excess entropy $S^{(2)}$ and the "cascade of anomalies" also applies for fluids of particles with short-range attractions relative to their diameter. This, and the relationship of the colloidal system's properties to liquid water's behavior, was first discussed in Ref. [16]. The excess entropy approach shows promise for application to molecular liquids. For example, the study of extended simple point charge (SPC/E) water shows that $S^{(2)}$ can capture the structural anomaly of water [3,15]. The scaling relation between the excess entropy and transport properties of different materials has also been investigated [17].

These findings suggest that the anomalous properties of water are closely related to its LDL-HDL structural changes. We propose that the excess entropy, as a measure of structure and correlation between particles, can predict the regions of structural, dynamic, and thermodynamic anomalies of water, and it can also predict the location of the Widom line. To test this proposal, we perform constant volume isothermal (*NVT*) molecular dynamics (MD) simulations of 512 TIP5P molecules [18]. The TIP5P water model is able to reproduce the thermodynamic properties of water over a broad region of the phase diagram, such as the temperature of maximum density of water around $T=277$ K at atmospheric pressure. The TIP5P model also has a second critical point in the accessible region of the phase diagram. Our simulations are performed using a cubic box with periodic boundary conditions. We control the temperature using a Berendsen thermostat.

Figure 1 shows the anomalous regions in the P-T phase diagram obtained from our MD simulation results. Our results are similar to results for the SPC/E water [3]. We compute D from the long-time behavior of the mean-square displacement of the water molecules $\langle r^2(t)\rangle$, using the Einstein relationship $6D=d\langle r^2(t)\rangle/dt$. We also compute the translational and orientational (tetrahedral) order parameters of water for different state points. Both order parameters have been widely used to investigate the structure of model liquids [3,9,14,19].

The excess entropy of water can be estimated from the two-body contribution $S^{(2)}$ arising in the expansion of the entropy in terms of partial N-body distribution functions using structural information in the form of oxygen-oxygen (O-O) pair correlation function (PCF) $g(r)$ [8,14,20],

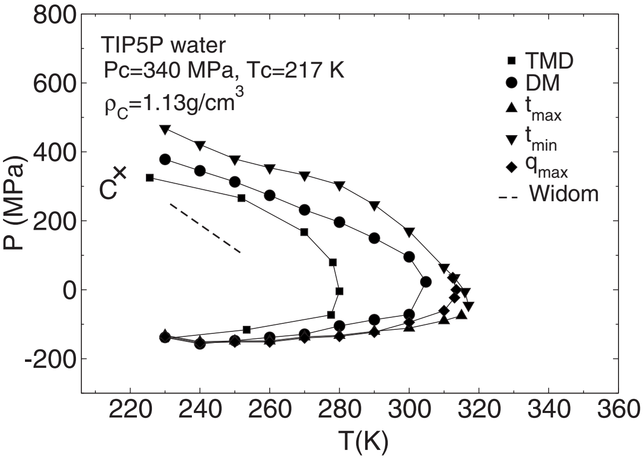

FIG. 1. Three regions of the TIP5P phase diagram obtained from our MD simulations. Data from Ref. [9]. Density anomaly region is defined by temperature of maximal density (TMD) line, inside which the density increases when the system is heated at constant pressure. Diffusion anomaly region is defined by the loci of diffusivity maxima-minima (DM), inside which the diffusivity increases with density at constant T. The structural anomaly region is defined by the loci of translational order minima ($t_{\rm min}$, ▼) and maxima ($t_{\rm max}$, ▲), or orientational order maxima $q_{\rm max}$ (◆), inside which both translational and orientational orders decrease with density at constant T (see Refs. [3,9] for details). The dashed line (Widom line) is the loci of the response function maximum (specific heat C_P). C is the hypothesized liquid-liquid critical point according to simulations of Ref. [18].

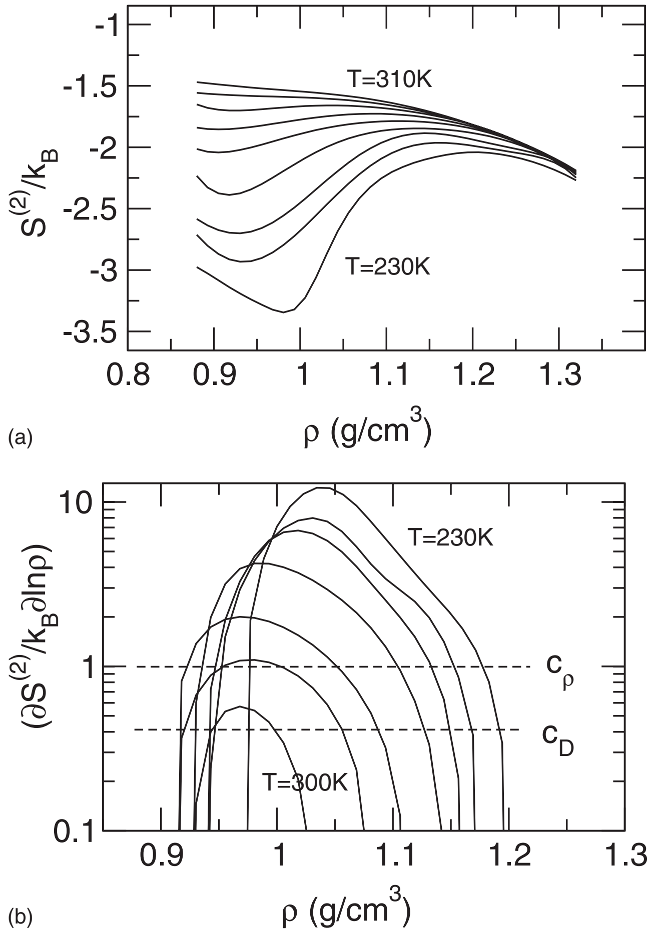

FIG. 2. Excess entropy of the TIP5P model of water $S^{(2)}$. (a) Temperature and density dependence of $S^{(2)}$. From bottom to top, the isotherms correspond to $T=230,240,250,260,270,280,290,300,310$ K. (b) Temperature and density dependence of $(\frac{\partial S^{(2)}}{\partial \ln \rho})_T$. From top to bottom, the isotherms correspond to $T=230,240,250,260,270,280,290,300$ K. The horizontal lines indicate the values of $(\frac{\partial S^{(2)}}{\partial \ln \rho})_T$ above which there is anomalous behavior of ρ and D, respectively [see discussion below Eq. (7)]. Note that $(\frac{\partial S^{(2)}}{\partial \ln \rho})_T$ is plotted in a logarithmic scale. Therefore only positive values can be seen, so the curve for $T=310$ K is not shown.

$$S_{\rm ex} \approx S^{(2)} = -2\pi\rho k_B \int \{g(r)\ln[g(r)] - [g(r)-1]\} r^2 dr, \tag{2}$$

and it can estimate the excess entropy to a reasonable level of accuracy for different model liquids [21–23]. For example, for the Lennard-Jones system [21], this two-body contribution to the excess entropy is between 85% and 95% over a fairly wide range of densities. It also captures the structural anomaly of liquid silica [14] and SPC/E water [15].

The main change of $g(r)$ of water upon compression occurs in the range of the second coordination shell [2], where water molecules migrate from the second shell toward the first shell. If the value of $g(r)$ is close to 1, we can write that $\ln[g(r)] \approx \ln[1+g(r)-1] \approx g(r)-1$. Thus from Eq. (2),

$$S^{(2)} \approx -2\pi\rho k_B \int \{g(r)[g(r)-1] - [g(r)-1]\} r^2 dr \tag{3}$$

$$\approx -2\pi\rho k_B \int [g(r)-1]^2 r^2 dr. \tag{4}$$

Expression (4) is similar to the translational order parameter $t \equiv \int |g(r)-1| dr$ [3,24], which quantifies the degree to which a water molecule and its nearest neighbors adopt preferential separations. This similarity is the reason why $S^{(2)}$ and t show similar anomalies for waterlike model liquids [3,8,9,14,19,24].

We compute $S_{\rm ex}$ using Eq. (2). Figure 2(a) shows the temperature and density dependence of $S_{\rm ex}$ of TIP5P water, qualitatively reproducing the result for SPC/E water [15]. $S_{\rm ex}$ shows normal behavior for $T > 300$ K when it decreases with density. Below $T=300$ K, $S_{\rm ex}$ develops anomalous behavior, increasing with density in an interval of density which widens upon cooling. This behavior is associated with the continuous change of structure upon compression and heating from the LDL-like local structure (open tetrahedral structure with low density, low entropy, and low energy) to the HDL-like local structure (more closed structure with high density, high entropy, and high energy) [2]. The anomalous change of $S_{\rm ex}$ is related to the density anomaly due to the negative thermal expansion coefficient, arising from the relation

$$kTV\alpha_P = \langle \delta V \delta S \rangle, \tag{5}$$

which predicts anticorrelation between the entropy and volume fluctuations. The S_{ex} anomaly is also related to the anomalous diffusivity increase with density due to the Adam-Gibbs equation

$$D \propto \exp[-B/(TS_c)], \tag{6}$$

where S_c is the configurational entropy [25].

Reference [8] has shown that in order to have waterlike density and diffusivity anomalies, $(\frac{\partial S_{\mathrm{ex}}}{\partial \ln \rho})_T$ needs to be larger than some specific value. Due to the Maxwell relation, the density anomaly $(\frac{\partial \rho}{\partial T})_P > 0$ is equivalent to the entropy anomaly $(\frac{\partial S}{\partial \rho})_T > 0$. Thus from the definition of excess entropy in Eq. (1), it follows that $(\frac{\partial S_{\mathrm{ex}}}{\partial \ln \rho})_T > ck_B$ with $c=1$. From the empirical Rosenfeld scaling relationship between diffusivity and excess entropy $D\frac{\rho^{1/3}}{T^{1/2}} = 0.6\exp(0.8S_{\mathrm{ex}}/k_B)$ established for various liquids [17], it follows that $(\frac{\partial S_{\mathrm{ex}}}{\partial \ln \rho})_T > ck_B$ with $c=0.42$ is a necessary condition for the diffusion anomaly.

Therefore, the condition to have density and diffusivity anomalies can be written as

$$\left(\frac{\partial S_{\mathrm{ex}}}{\partial \ln \rho}\right)_T > ck_B, \tag{7}$$

where for the density anomaly $c=c_\rho=1$, and for the diffusivity anomaly $c=c_D=0.42$ [8]. For the two-scale ramp liquid [8], the behavior of $S^{(2)}$ is similar to the behavior of S_{ex} with respect to their changes with density. Moreover the region of anomalies predicted by $S^{(2)}$ for ramp model is in agreement with the results obtained by MD simulation. It is known that two-scale ramp potential can reproduce waterlike density and diffusion anomalies [9]. Thus we assume that we can use $S^{(2)}$ to predict anomalies of water instead of S_{ex}. To predict the regions of density and diffusivity anomalies, we show density and temperature dependence of $(\frac{\partial S^{(2)}}{k_B \partial \ln \rho})_T$ in Fig. 2(b). The anomalous regions for density and diffusivity can be identified by finding the range of density between which the value of $(\frac{\partial S^{(2)}}{k_B \partial \ln \rho})_T$ for different T is greater than c_ρ or c_D, respectively.

Figures 3(a) and 3(b) compare the regions of anomalies for density and diffusivity, respectively, in the T-ρ plane with the predictions of Eq. (7) (open symbols). Figure 3(c) compares the regions of the structural anomaly quantified by the anomalous behavior of S_{ex} and the order parameters t and q obtained from MD simulations. These results suggest that for water the two-body contribution $S^{(2)}$ captures most of the change of the excess entropy with density. Thus we conjecture that the three-body and higher-body terms have small changes with density. These results indicate that Eq. (7) not only relates the behavior of the excess entropy to the anomalies in a spherically symmetric ramp model [8], but also applies to water. It would be interesting to test the results of our simulations using experimental data on the O-O PCF for a range of temperatures and densities.

Near the critical point, the total correlation function $h(r) \equiv g(r)-1$ has the asymptotic behavior for $r \to \infty$ [26],

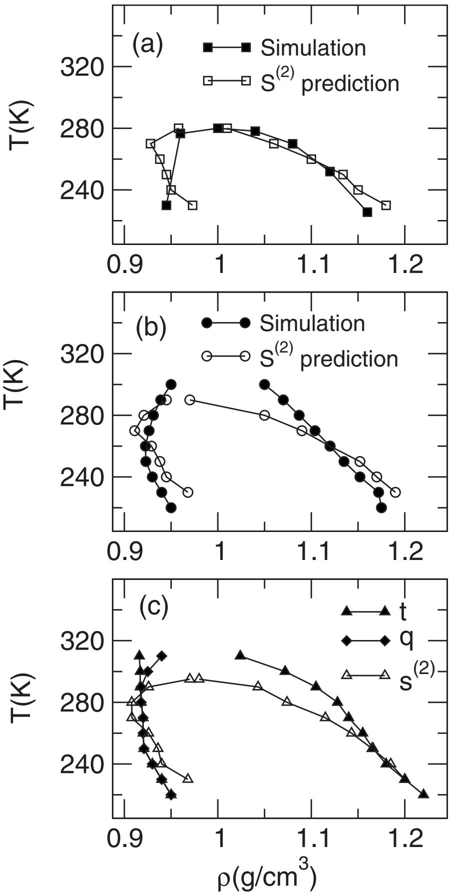

FIG. 3. Comparison of the boundaries of anomalous regions with the prediction based on the excess entropy calculation within T-ρ plane for TIP5P water. (a) Density anomaly region. (b) Diffusion anomaly region. Filled symbols are results based on MD simulations and open symbols are results based on the prediction of Eq. (7). (c) Comparison of the loci of excess entropy extrema from Fig. 2 with the structural anomaly regions found by MD simulations. The open triangles denote the loci of excess entropy $S^{(2)}$ extrema. The filled triangles denote the loci of extrema of translational order t. The filled diamonds denote loci of maxima of orientational order q.

$$h(r) \sim r^{-(d-2+\eta)} \exp(-r/\xi), \tag{8}$$

where ξ is the correlation length, d is the dimension (3 in our case) and $\eta \approx 0$ is correlation function decay exponent. Hence using Eq. (8), we can rewrite Eq. (4) as

$$S^{(2)} \approx -2\pi\rho \int |h(r)|^2 r^2 dr \tag{9}$$

$$\sim -2\pi\rho \int \exp(-2r/\xi) dr = -\pi\rho\xi. \tag{10}$$

We find

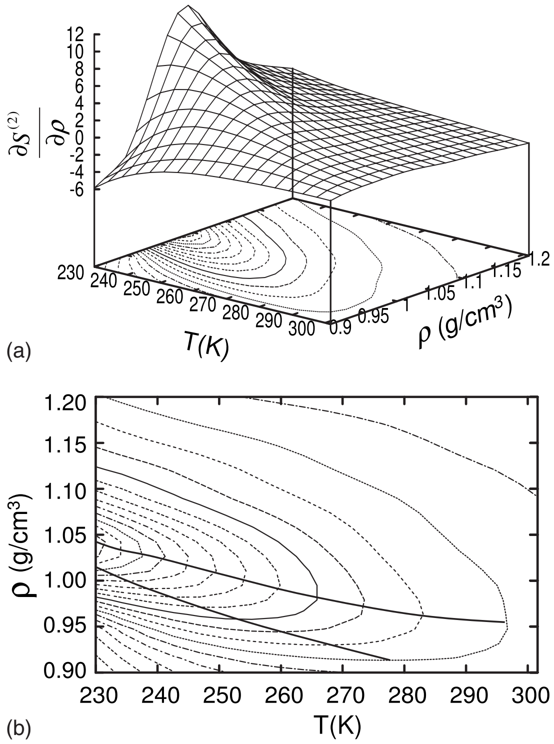

FIG. 4. (a) The three-dimensional plot shows the temperature and density dependence of $(\frac{\partial S^{(2)}}{\partial \rho})_T$ with the contour plot projected on the T-ρ plane. There is a locus of the maximum in $(\frac{\partial S^{(2)}}{\partial \rho})_T$ along the constant-T path and constant-ρ path. (b) The two-dimensional contour plot of $(\frac{\partial S^{(2)}}{\partial \rho})_T$ shows that the locus of its maximum forms two lines (the bold lines) along constant-T path and constant-ρ path, respectively.

$$\left(\frac{\partial S^{(2)}}{\partial \rho}\right)_T \sim \xi + \rho\left(\frac{\partial \xi}{\partial \rho}\right)_T = \xi + \rho\left(\frac{\partial \xi}{\partial P}\right)_T\left(\frac{\partial P}{\partial \rho}\right)_T. \qquad (11)$$

Near the critical point of fluids, the scaling law between P and ρ can be expressed as $|P-P_c| = A|\rho-\rho_c|^{\delta}$, where A is constant, P_c and ρ_c are critical pressure and density, and $\delta \approx 5$ is the critical exponent [26]. Therefore, the term $(\frac{\partial P}{\partial \rho})_T \propto |\rho-\rho_c|^4 \rightarrow 0$ upon approaching ρ_c. Equation (11) suggests that we can estimate the Widom line of water by finding the maximum of $(\frac{\partial S^{(2)}}{\partial \rho})$, since the Widom line corresponds to the locus of maxima of the correlation length.

Figure 4(a) shows that $(\frac{\partial S^{(2)}}{\partial \rho})_T$ as a function of density and temperature reaches a maximum at a specific density $\rho_{\text{max}}(T)$ along a fixed T path, or reaches a maximum at a specific temperature $T_{\text{max}}(\rho)$ along a fixed ρ path. The contour plot of $(\frac{\partial S^{(2)}}{\partial \rho})_T$ in Fig. 4(b) predicts two lines corresponding to the loci of maxima in $(\frac{\partial S^{(2)}}{\partial \rho})_T$ along constant-T and constant-ρ paths. These two (bold) lines asymptotically approach each other as they come closer to the critical point. The common asymptote provides a quantitative prediction of the Widom line based on the excess entropy. Therefore, the excess entropy computed from the O-O PCF can predict the location of the Widom line and therefore the approximate location of other response function maxima, such as C_P and K_T.

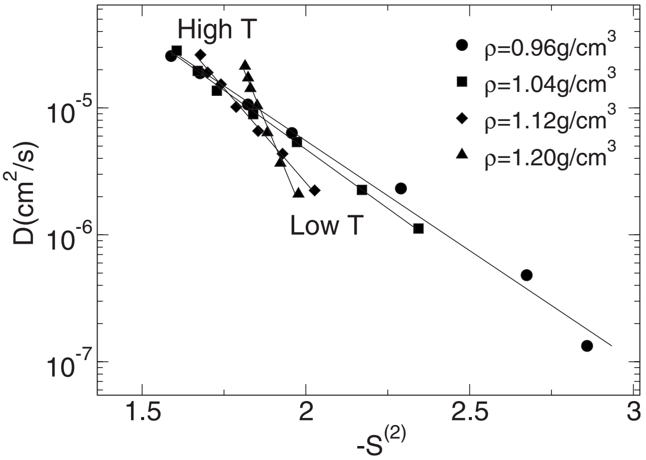

FIG. 5. The relation between diffusivity and the negative of the excess entropy of water along isochores. The temperature range for each density is 240–300 K.

The excess entropy can also predict the location of the dynamic transition from fragile to strong behavior in supercooled water [4]. The relationship between configurational entropy S_c and diffusivity D of water is known to be well approximated by the Adam-Gibbs equation (6). A different relation between S_{ex} and D was proposed for waterlike core-softened repulsive simple potential liquid, binary Lennard-Jones alloy [27] and SPC/E water [15],

$$D(T) \propto \exp[b(\rho)S_{\text{ex}}], \qquad (12)$$

where $b(\rho)$ is a T-independent parameter and ρ is constant. Our calculation (Fig. 5) confirms these results for the TIP5P water.

In summary, our MD study using the TIP5P shows that two-body excess entropy, obtained from the O-O PCF, can be used to predict the thermodynamic and dynamic properties of water, and it can also estimate the location of the LDL-HDL Widom line. Our results imply that it is possible to estimate the thermodynamic and dynamic anomalies of liquid from the structural change, and it is also possible to relate structural change to the correlation length maximum and therefore the hypothesized LDL-HDL critical point.

We thank NSF Chemistry program for support. SVB thanks the Office of the Academic Affairs of Yeshiva University for funding the Yeshiva University high-performance computer cluster and acknowledges the partial support of this research through the Dr. Bernard W. Gamson Computational Science Center at Yeshiva College.

---

[1] P. H. Poole, F. Sciortino, U. Essmann, and H. E. Stanley, Nature (London) **360**, 324 (1992).

[2] A. K. Soper and M. A. Ricci, Phys. Rev. Lett. **84**, 2881 (2000).

[3] J. R. Errington and P. G. Debenedetti, Nature (London) **409**, 318 (2001).

[4] L. Xu, P. Kumar, S. V. Buldyrev, S.-H. Chen, P. H. Poole, F. Sciortino, and H. E. Stanley, Proc. Natl. Acad. Sci. U.S.A. **102**, 16558 (2005); L. Xu, S. V. Buldyrev, C. A. Angell, and H. E. Stanley, Phys. Rev. E **74**, 031108 (2006).

[5] Figures 4 and 6 of F. Sciortino, P. H. Poole, U. Essmann, and H. E. Stanley, Phys. Rev. E **55**, 727 (1997); Figs. 5 and 6 of S. Harrington P. H. Poole, F. Sciortino, and H. E. Stanley, J. Chem. Phys. **107**, 7443 (1997); Fig. 2 of P. H. Poole, I. Saika-Voivod, and F. Sciortino, J. Phys.: Condens. Matter **17**, L431 (2005).

[6] S. H. Chen F. Mallamace, C.-Y. Mou, M. Broccio, C. Corsaro, and A. Faraone, Proc. Natl. Acad. Sci. U.S.A. **103**, 12974 (2006); P. Kumar, S. V. Buldyrev, S. L. Becker, P. H. Poole, F. W. Starr, and H. E. Stanley, *ibid.* **104**, 9575 (2007).

[7] P. C. Hemmer and G. Stell, Phys. Rev. Lett. **24**, 1284 (1970); G. Stell and P. C. Hemmer, J. Chem. Phys. **56**, 4274 (1972).

[8] J. R. Errington, T. M. Truskett, and J. Mittal, J. Chem. Phys. **125**, 244502 (2006).

[9] Z. Yan, S. V. Buldyrev, N. Giovambattista, and H. E. Stanley, Phys. Rev. Lett. **95**, 130604 (2005); Z. Yan, S. V. Buldyrev, N. Giovambattista, P. G. Debenedetti, and H. E. Stanley, Phys. Rev. E **73**, 051204 (2006); Z. Yan, S. V. Buldyrev, P. Kumar, N. Giovambattista, P. G. Debenedetti, and H. E. Stanley, *ibid.* **76**, 051201 (2007); Z. Yan, S. V. Buldyrev, P. Kumar, N. Giovambattista, and H. E. Stanley, *ibid.* **77**, 042201 (2008). See also, M. Canpolat, F. W. Starr, M. R. Sadr-Lahijany, A. Scala, O. Mishima, S. Havlin, and H. E. Stanley, Chem. Phys. Lett. **294**, 9 (1998).

[10] M. R. Sadr-Lahijany, A. Scala, S. V. Buldyrev, and H. E. Stanley, Phys. Rev. Lett. **81**, 4895 (1998); Phys. Rev. E **60**, 6714 (1999); A. Scala, M. R. Sadr-Lahijany, N. Giovambattista, S. V. Buldyrev, and H. E. Stanley, *ibid.* **63**, 041202 (2001); J. Stat. Phys. **100**, 97 (2000).

[11] G. Franzese, G. Malescio, A. Skibinsky, S. V. Buldyrev, and H. E. Stanley, Nature (London) **409**, 692 (2001); Phys. Rev. E **66**, 051206 (2002); A. Skibinsky, S. V. Buldyrev, G. Franzese, G. Malescio, and H. E. Stanley, *ibid.* **69**, 061206 (2004); G. Malescio, G. Franzese, A. Skibinsky, S. V. Buldyrev, and H. E. Stanley, *ibid.* **71**, 061504 (2005).

[12] E. A. Jagla, Phys. Rev. E **58**, 1478 (1998); J. Chem. Phys. **111**, 8980 (1999); Phys. Rev. E **63**, 061509 (2001). S. V. Buldyrev, G. Franzese, N. Giovambattista, G. Malescio, M. R. Sadr-Lahijany, A. Scala, A. Skibinsky, and H. E. Stanley, Physica A **304**, 23 (2002).

[13] A. B. Oliveira, G. Franzese, P. A. Netz, and M. C. Barbosa, J. Chem. Phys. **128**, 064901 (2008).

[14] R. Sharma, S. N. Chakraborty, and C. Chakravarty, J. Chem. Phys. **125**, 204501 (2006).

[15] J. Mittal, J. R. Errington, and T. M. Truskett, J. Phys. Chem. B **110**, 18147 (2006).

[16] W. P. Krekelberg, J. Mittal, V. Ganesan, and T. M. Truskett, J. Chem. Phys. **127**, 044502 (2007); Phys. Rev. E **77**, 041201 (2008).

[17] Y. Rosenfeld, J. Phys.: Condens. Matter **11**, 5415 (1999).

[18] M. Yamada, S. Mossa, H. E. Stanley, and F. Sciortino, Phys. Rev. Lett. **88**, 195701 (2002); D. Paschek, *ibid.* **94**, 217802 (2005).

[19] M. S. Shell, P. G. Debenedetti, and A. Z. Panagiotopoulos, Phys. Rev. E **66**, 011202 (2002).

[20] R. E. Nettleton and M. S. Green, J. Chem. Phys. **29**, 1365 (1958).

[21] A. Baranyai and D. J. Evans, Phys. Rev. A **40**, 3817 (1989).

[22] J.-L. Bretonnet, J. Chem. Phys. **117**, 9370 (2002).

[23] I. Yokoyama, Physica B **269**, 244 (1999).

[24] T. M. Truskett, S. Torquato, and P. G. Debenedetti, Phys. Rev. E **62**, 993 (2000).

[25] A. Scala, F. W. Starr, E. La Nave, F. Sciortino, and H. Eugene Stanley, Nature (London) **406**, 166 (2000).

[26] J. P. Hansen and I. R. McDonald, *Theory of Simple Liquids* (Academic, London, 1986).

[27] J. Mittal, J. R. Errington, and T. M. Truskett, J. Chem. Phys. **125**, 076102 (2006).